

A Control Scheme Using Kalman Filter and Linear Quadratic Regulator for Power Quality Conditioning Devices

L.Sreedivika¹, B.Bhagyamma²

¹ PG Scholar, Department of EEE, JNTU Anantapur, Andhra Pradesh, India

² PG Scholar, Department of EEE, JNTU Anantapur, Andhra Pradesh, India

Abstract— This contribution shows how the Kalman filter (KF) and linear quadratic regulator (LQR) can be used for improving the power quality conditioning devices. Grid perturbations such as load variations, frequency deviation, voltage distortion, line impedance, unbalance, and measurement noise are taken into account. The design principles and the validity of the model have been outlined. The control system is based on the Kalman filter (KF), which estimates the state space variables at the point of common coupling. Generating the references for the controller is also responsible for this algorithm. Performance of the control system is verified by applying the method to shunt active power filter and series active power filter.

Keywords— Active power filter, Kalman filter, linear quadratic regulator (LQR), optimum control, optimum filtering, power quality, reference generation.

1. INTRODUCTION

The quality of electrical power supply is assessed by a set of parameters which describe the process of electrical power delivery to the user under normal operating conditions. When the voltage or current deviates significantly from its normal or ideal wave shape, these sudden deviations are called events. Power quality events are the phenomena which can lead to tripping of equipment, to interruption of the production or of plant operation, or endanger power system operation. This includes interruptions, under voltage, over voltage, phase angle jumps and three phase unbalance. PQCDs are a possible alternative to minimize the nonlinear effects of the loads on the power system, Active power filters and battery energy storage devices are examples of such conditioning devices.[1] The most common approach to design the controllers for this kind of equipment is to consider the output filter of the devices as the plant to be controlled. The load dynamics and the line impedances are usually neglected and are considered perturbations in the mathematical model of the plant. As a consequence, the controller must be able to reject such perturbations and ensure that the power conditioner behaves adequately under a dynamic standpoint. Depending on the nature of the disturbances, however, the overall system may oscillate and even

become unstable. These effects have been reported in the literature [2].

Line impedance is also responsible for the voltage distortion caused by the circulation of non-sinusoidal current. It degrades the performance of the power conditioners due to its effects on the corresponding control and synchronization systems [3]-[4]. A new preliminary modelling methodology was introduced where a more realistic model applied for grid connected systems is presented while considering the dynamics of the distorted point of common coupling (PCC) voltages. This approach was shown to be an improved alternative using linear quadratic regulator (LQR) controllers and the Kalman filter (KF) algorithm [5] applied to these systems. The KF is a recursive algorithm that is well known for dealing with dynamic systems corrupted by uncertainties or noise and which has been widely studied and used in very different applications [6].

In addition to the controller, the reference generation plays an important role to achieve the compensation objectives [7]–[9]. It is assumed that the frequency of the grid is constant, and only harmonics are detected. In a recent paper [10], a mathematical model that is capable of identifying harmonics and unbalance is proposed while using a KF with less computational effort. The method is based on single phase filter. However, this method still considers a constant frequency and the model is derived by rotating axes, which leads to a time-variant model even under constant frequency, in contrast with the time invariant model used in this work. In the time variant model, it would also need an extra block for proper synchronization that is not the case in this proposal.

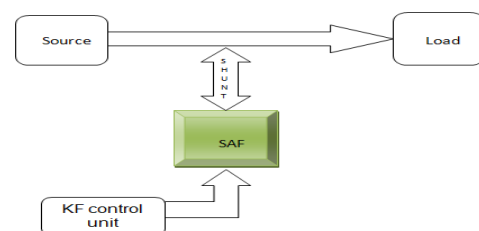


Fig. 1. Kalman filter-based control system for a power quality conditioning device.

Time invariance is an important property of the proposed model that leads to a simplification corresponding to a reduction of the computational effort required in digital implementations as described in [11]. This paper focuses on the control system for power quality conditioning device (PQCD), and two main subjects are taken into account:

- 1) Minimizing the effects of the voltage at the PCC on the performance of the PQCD by designing an adequate controller;
- 2) Developing auxiliary algorithms based on the KF for reference generation that can cope with several grid perturbations such as: frequency variation, measurement noise, continuous variable power level of the load.

2. DESCRIPTION OF THE PROPOSAL

The PQDCs considered in this paper are shunt active power filter and series active power filter. The shunt active power filter is composed by a DC link and a three phase IGBT inverter followed by an inductive output filter. The proposed method is depicted in Fig. 1. The system is designed to inject a current into the line such as to compensate the harmonic content of the load. The compensation must be considered under several perturbations on the grid, such as measurement noise, current or voltage transients, frequency deviation, and the inherent voltage perturbation at the PCC that affects the dynamic behaviour of the SAF. To achieve that, the system is controlled by a KF-based control structure that is the scope of this paper.

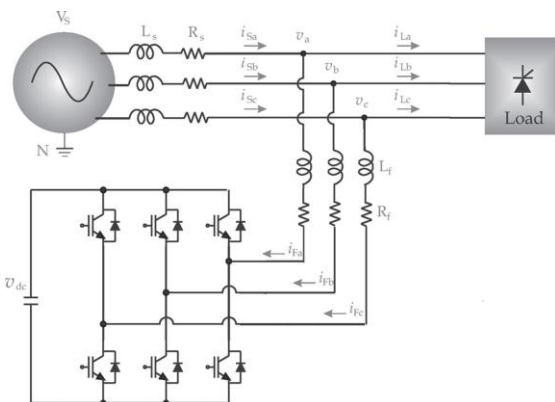


Fig. 2. Electric diagram of the SAF.

The control system uses the measurements of the load currents (I_{Labc}), SAF currents (I_{Fabc}) and voltages at the PCC (V_{abc}). A KF algorithm is then used to extract harmonic and quadrature components of I_{Labc} and V_{abc} . These components are used to generate the references for current compensation and also to estimate the harmonic components of voltage at the PCC and their corresponding derivatives.

3. MODEL OF THE PLANT

A. Conventional Model

The schematic diagram of the SAF is shown in Fig. 2. Based on the diagram in that figure and in accordance with [12], the plant model in the dq frame is given by

$$\dot{i}_{dq} = A i_{dq} + B d_{dq} + C v_{dq} \tag{1}$$

$$y_{dq} = C i_{dq} \tag{2}$$

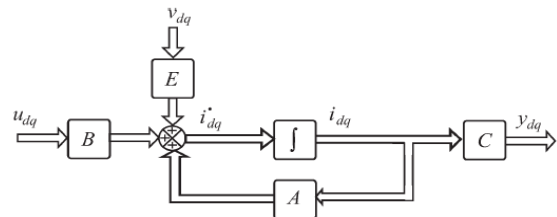


Fig.3. System representation, considering the grid voltage as a disturbance.

Where

$$A = \begin{bmatrix} R_f & -\omega \\ L_f & R_f \\ \omega & L_f \end{bmatrix}$$

$$B = \begin{bmatrix} v_{dc} & 0 \\ L_f & v_{dc} \\ 0 & L_f \end{bmatrix}$$

$$E = \begin{bmatrix} 1 & 0 \\ L_f & 1 \\ 0 & L_f \end{bmatrix}$$

$$C = \begin{bmatrix} 1 & 0 \\ 0 & 1 \end{bmatrix}$$

and d_{dq} is the switching function vector.

It may be seen by (1) that this approach considers the voltage at the PCC as a disturbance added to the system. Fig. 3 shows the plant according to this representation.

B. Proposed Mathematical Model

In order to consider the dynamics inserted in the system by the unknown line impedance, which are reflected at the PCC voltage dynamics, a new modelling scheme. In this new modelling approach, the dynamics of the PCC voltage is included in the plant model. The model that represents the fundamental voltage disturbance, at the PCC of the power conditioning system, in the dq frame is given by (see Appendix A)

$$\begin{bmatrix} \dot{v}_d \\ v_q \\ \dot{v}_d \\ \dot{v}_q \end{bmatrix} = M_{4 \times 4}^{dq} \begin{bmatrix} v_d \\ v_q \\ \dot{v}_d \\ \dot{v}_q \end{bmatrix} \quad (3)$$

With

$$M_{4 \times 4}^{dq} = \begin{bmatrix} 0 & 0 & 1 & 0 \\ 0 & 0 & 0 & 1 \\ -\omega^2 & 0 & 0 & \omega \\ 0 & -\omega^2 & -\omega & 0 \end{bmatrix}$$

The complete rotating reference frame model of the considered system may be written as

$$\begin{bmatrix} \dot{i}_d \\ i_q \\ v_d \\ v_q \\ \dot{v}_d \\ \dot{v}_q \end{bmatrix} = \bar{A} \begin{bmatrix} i_d \\ i_q \\ v_d \\ v_q \\ \dot{v}_d \\ \dot{v}_q \end{bmatrix} + \bar{B} \begin{bmatrix} d_d \\ d_q \end{bmatrix} \quad (4)$$

$$y_{dq} = \bar{C} \begin{bmatrix} i_d \\ i_q \\ v_d \\ v_q \\ \dot{v}_d \\ \dot{v}_q \end{bmatrix} \quad (5)$$

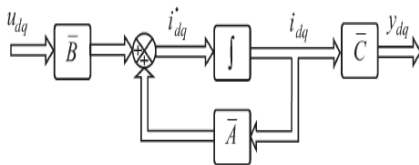


Fig. 4. System representation, considering the dynamics of the grid voltage as part of the model.

Where

$$\bar{A} = \begin{bmatrix} -\frac{R_f}{L_f} & \omega & \frac{1}{L_f} & 0 & 0 & 0 \\ -\omega & -\frac{R_f}{L_f} & 0 & \frac{1}{L_f} & 0 & 0 \\ 0 & 0 & 0 & 0 & 1 & 0 \\ 0 & 0 & 0 & 0 & 0 & 1 \\ 0 & 0 & -\omega^2 & 0 & 0 & \omega \\ 0 & 0 & 0 & -\omega^2 & -\omega & 0 \end{bmatrix}$$

$$\bar{B} = - \begin{bmatrix} \frac{v_{dc}}{L_f} & 0 \\ 0 & \frac{v_{dc}}{L_f} \\ 0 & 0 \\ 0 & 0 \\ 0 & 0 \\ 0 & 0 \end{bmatrix}$$

$$\bar{C} = \begin{bmatrix} 1 & 0 & 0 & 0 & 0 & 0 \\ 0 & 1 & 0 & 0 & 0 & 0 \end{bmatrix}$$

In order to consider the PCC voltages containing 'n' harmonic components, matrices \bar{A} , \bar{B} , and \bar{C} have to be modified to \bar{A}_n , \bar{B}_n , and \bar{C}_n , respectively, as presented in

$$\bar{A}_n = \begin{bmatrix} A & \frac{1}{L_f} & 0 & \dots & \frac{1}{L_f} \\ 0 & \frac{1}{L_f} & \dots & 0 & \frac{1}{L_f} \\ 0 & M_{4 \times 4}^{dq} & \dots & \dots & 0 \end{bmatrix}$$

$$\bar{B}_n = - \begin{bmatrix} \frac{v_{dc}}{L_f} & 0 \\ 0 & \frac{v_{dc}}{L_f} \\ 0 & 0 \\ \vdots & \vdots \\ 0 & 0 \end{bmatrix}$$

$$\bar{C}_n = \begin{bmatrix} 1 & 0 & 0 & 0 & \dots & 0 \\ 0 & 1 & 0 & 0 & \dots & 0 \end{bmatrix}$$

Where $M_{4n \times 4n}^{dq}$ is given in Appendix B.

4. CONTROLLER

In order to apply the LQR methodology, the plant must be described by

$$x_{k+1} = A_d x_k + B_d u_k \quad (6)$$

and

$$y_k = C_d x_k \quad (7)$$

where $dim\{x_k\} = n$ and $dim\{u_k\} = m$.

The LQR controller is given by

$$u_k = -K x_k \quad (8)$$

which minimises the cost function

$$J = \frac{1}{2} \sum_{k=0}^{\infty} \{ x_k^T Q_{n \times n}^{LQR} x_k + u_k^T R_{m \times m}^{LQR} u_k \} \quad (9)$$

Where $Q_{n \times n}^{LQR}$ is a positive semi definite matrix and $R_{m \times m}^{LQR}$ is a positive definite matrix.

The K gains can be obtained solving the algebraic Recatti equation.

$$P = A_d^T P (A_d - B_d K) + Q_{n \times n}^{LQR} \quad (10)$$

$$K = (B_d^T P B_d + R_{m \times m}^{LQR})^{-1} B_d^T P A_d \quad (11)$$

A. LQR_{KF} Controller Design

Therefore, the model may be depicted by the block diagram as shown in Fig. 4.

The LQR_{KF} compensator incorporates the PCC voltages in the model used to calculate the controller gain vector K , thus considering up to n odd harmonics in the PCC voltage signals and adding integral action in the closed-loop system. Eqn.(12) gives the new model used to calculate the gain vector K of the LQR_{KF} controller.

The structure of the LQR_{KF} controller is, therefore, shown in Fig. 5. It is possible to notice that this approach includes the whole system dynamics, with PCC voltage disturbance being compensated with the aid of information that comes from the KF. The estimation of the state space variables related to the PCC voltages needed by the controller and the generation of the current references will be discussed.

$$\begin{bmatrix} e_d \\ e_q \\ \int e_d \\ \int e_q \\ v_d^1 \\ v_q^1 \\ \dot{v}_d^1 \\ \dot{v}_q^1 \\ \vdots \\ v_d^n \\ v_q^n \\ \dot{v}_d^n \\ \dot{v}_q^n \end{bmatrix} = \bar{A}_{n1} \begin{bmatrix} e_d \\ e_q \\ \int e_d \\ \int e_q \\ v_d^1 \\ v_q^1 \\ \dot{v}_d^1 \\ \dot{v}_q^1 \\ \vdots \\ v_d^n \\ v_q^n \\ \dot{v}_d^n \\ \dot{v}_q^n \end{bmatrix} + \bar{B}_{n1} \begin{bmatrix} d_d \\ d_q \end{bmatrix} \quad (12)$$

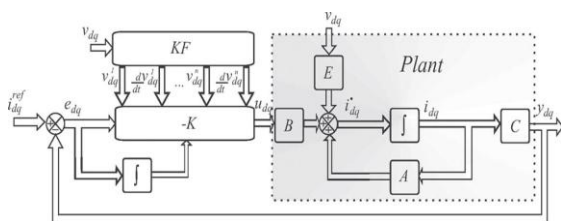


Fig.5. LQR_{KF} servo-system structure.

Where

$$\bar{A}_{n1} = \begin{bmatrix} A_1 & \frac{1}{L_f} & 0 & \dots & \frac{1}{L_f} \\ 0 & \frac{1}{L_f} & \dots & 0 & \frac{1}{L_f} \\ 0 & M_{4 \times 4}^{dq} & \dots & \dots & 0 \end{bmatrix}$$

$$\bar{B}_{n1} = - \begin{bmatrix} \frac{v_{dc}}{L_f} & 0 \\ 0 & \frac{v_{dc}}{L_f} \\ 0 & 0 \\ \vdots & \vdots \\ 0 & 0 \end{bmatrix}$$

$$A_1 = \begin{bmatrix} -\frac{R_f}{L_f} & \omega & 0 & 0 \\ -\omega & -\frac{R_f}{L_f} & 0 & 0 \\ 0 & 0 & 1 & 0 \\ 0 & 0 & 0 & 1 \end{bmatrix}$$

and $M_{4n \times 4n}^{dq}$ is obtained by applying (52).

B .LQR Controller

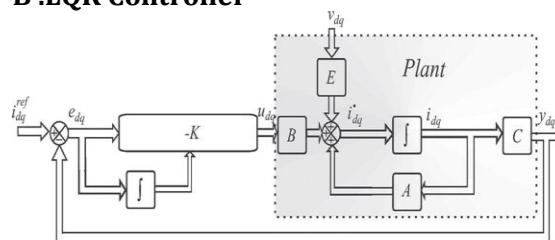


Fig.6. LQR servo-system structure.

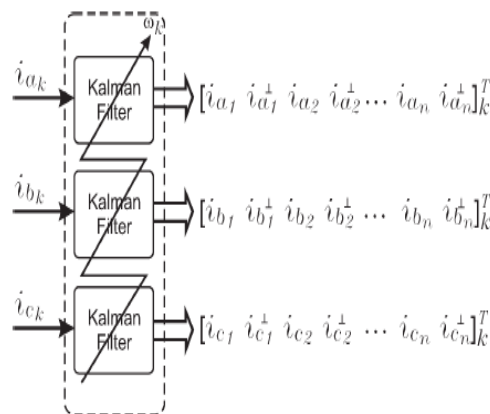


Fig.7. Representation of the Kalman filter harmonic decomposition.

5. REFERENCE GENERATION AND ESTIMATION OF THE PCC STATE SPACE VARIABLES

The KF-PLL is composed by a block responsible to extract the harmonic content of a signal, a positive sequence extractor, and a phase detector. It also detects the frequency of the grid. Frequency identification is its main advantage over other similar approaches that consider constant frequency. The blocks of the KF-PLL are used to generate the references for the controller and to estimate the PCC voltage state space variables, as described below. In this section, the subscript j can assume the values $a, b,$ or c indicating that the equation is valid for the three phases.

A. Harmonic Estimation

The mathematical model of the signal to be filtered must incorporate the harmonics that are to be canceled. Defining the relationship between the states of the filter and the filtered quantities, that is,

$$\begin{bmatrix} \hat{x}_{j_1} & \hat{x}_{j_2} & \hat{x}_{j_3} & \hat{x}_{j_4} & \dots & \hat{x}_{j_{2n-1}} & \hat{x}_{j_{2n}} \end{bmatrix}^T_{k/k-1} \Leftrightarrow \begin{bmatrix} i_{j_1} & i_{j_1}^\perp & i_{j_2} & i_{j_2}^\perp & \dots & i_{j_n} & i_{j_n}^\perp \end{bmatrix}^T_k \quad (13)$$

Where the symbol \perp indicates the quadrature estimated component.

The selective harmonic reference generation is directly obtained. This is,

$$i_{j_{1k}}^{ref} = \sum_{m=2,3,\dots} i_{j_{mk}} \quad (14)$$

Another approach is to estimate the fundamental current and extract it from the measured value of the current

$$i_{j_{1k}}^{ref} = i_{j_k} - i_{j_{1k}} \quad (15)$$

The KF uses the fundamental grid frequency in the mathematical model of the process to be filtered, and this frequency must be updated. Therefore, provided that $A_{i_{a_{1k}}} \neq 0$, the sinusoidal driving signal r_{ω_k} used in

the frequency identifier [11] can be obtained from the normalization of the fundamental signal.

$$r_{\omega_k} = \frac{i_{a_{1k}}}{A_{i_{a_{1k}}}} \quad (16)$$

$$A_{i_{a_{1k}}} = \sqrt{(i_{a_{1k}})^2 + (i_{a_{1k}}^\perp)^2} \quad (17)$$

B. Unbalance Detection

It is necessary to compensate the negative sequence and/or the zero sequence of the fundamental current. The determination of the positive sequence is obtained by [12],

$$\begin{bmatrix} i_{a_k}^+ \\ i_{b_k}^+ \\ i_{c_k}^+ \end{bmatrix} = \frac{1}{3} \begin{bmatrix} 1 & \alpha & \alpha^2 \\ \alpha^2 & 1 & \alpha \\ \alpha & \alpha^2 & 1 \end{bmatrix} \begin{bmatrix} i_{a_{1k}} \\ i_{b_{1k}} \\ i_{c_{1k}} \end{bmatrix} \quad (18)$$

Where $\alpha = e^{j120^\circ}$. Defining the 90° phase-shift operator e^{j90° and considering

$$\alpha = -\left(\frac{j}{2}\right) \pm \left(\frac{\sqrt{3}}{2}\right)e^{j90^\circ} \text{ then, (18) becomes}$$

$$i_{a_k}^+ = \frac{1}{3} i_{a_{1k}} - \frac{j}{6} (i_{b_{1k}} + i_{c_{1k}}) + \frac{\sqrt{3}}{6} (i_{b_{1k}}^\perp - i_{c_{1k}}^\perp),$$

$$i_{b_k}^+ = -i_{a_k}^+ - i_{c_k}^+,$$

$$i_{c_k}^+ = \frac{1}{3} i_{c_{1k}} - \frac{j}{6} (i_{b_{1k}} + i_{a_{1k}}) + \frac{\sqrt{3}}{6} (i_{b_{1k}}^\perp - i_{a_{1k}}^\perp) \quad (19)$$

The fundamental values $i_{a_{1k}}, i_{b_{1k}}, i_{c_{1k}}$ and their 90° shifted values $i_{a_{1k}}^\perp, i_{b_{1k}}^\perp, i_{c_{1k}}^\perp$ are obtained from the KFs used to generate the harmonics references. The reference for unbalance compensation is

$$i_{j_{1k}}^{ref} = i_{j_{1k}} - i_{j_{1k}}^+ \quad (20)$$

The signal r_{ω_k} used by the frequency identifier can be evaluated by (16).

C. Displacement Power Factor Detection without Unbalance Compensation

Based on Fig. 8, the following voltage and current definitions can be applied

$$\begin{aligned} v_{j_{1k}} &= A_{v_{j_{1k}}} \sin(\omega_k t_k + \theta_{v_{j_{1k}}}) = A_{v_{j_{1k}}} \sin(\phi_{v_{j_{1k}}}) \\ i_{j_{1k}} &= A_{i_{j_{1k}}} \sin(\omega_k t_k + \theta_{i_{j_{1k}}}) = A_{i_{j_{1k}}} \sin(\phi_{i_{j_{1k}}}). \end{aligned} \quad (21)$$

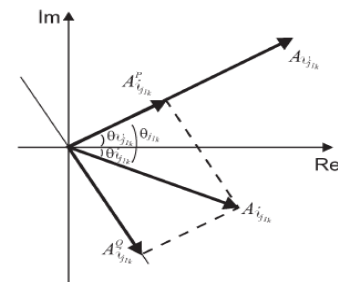


Fig.8. Relations to obtain the fundamental reactive current.

The angle between the voltage and current is

$$\theta_{j_{1k}} = \phi_{i_{j_{1k}}} - \phi_{v_{j_{1k}}} = \theta_{i_{j_{1k}}} - \theta_{v_{j_{1k}}}. \quad (22)$$

To obtain the angle $\theta_{j_{1k}}$ two KFs are used. The first one is the filter used to generate the harmonic current references. The second one uses the phase voltage measurements at PCC. This second filter will also be used to estimate the PCC state space variables.

The instantaneous phase of the currents and voltages is evaluated by

$$\phi_{i_{j_{1k}}} = \arctan\left(\frac{i_{j_{1k}}}{i_{j_{1k}}^\perp}\right) \quad \phi_{v_{j_{1k}}} = \arctan\left(\frac{v_{j_{1k}}}{v_{j_{1k}}^\perp}\right). \quad (23)$$

Based on the Eqns. (22) and (23), the angle between voltage and current is determined. Then, the instantaneous fundamental reactive current of the load is given by

$$i_{j1k}^Q = A_{ij1k}^Q \cos(\phi_{vj1k}) \quad (24)$$

where its amplitude is given by

$$A_{ij1k}^Q = A_{ij1k} \sin(\theta_{j1k}) \quad (25)$$

Note that

$$A_{ij1k} = \sqrt{(i_{j1k}^-)^2 + (i_{j1k}^+)^2} \quad (26)$$

Given a desired DPF, the amplitude of the fundamental reactive current associated is

$$A_{ij1k}^{Qd} = \pm A_{ij1k} \cos(\theta_{j1k}) \tan(\arccos(\text{DPF}_{j1k})) \quad (27)$$

Where A_{ij1k}^{Qd} is positive if i_{j1k} leads v_{j1k} , and it is negative if

i_{j1k} lags v_{j1k} . This equation gives the desired compensated fundamental reactive current

$$i_{j1k}^{Qd} = A_{ij1k}^{Qd} \cos(\phi_{vj1k}). \quad (28)$$

Therefore, from (22), (24) and (28), the fundamental reactive current reference is

$$i_{j1k}^{Qref} = (A_{ij1k}^Q - A_{ij1k}^{Qd}) \cos(\phi_{vj1k}). \quad (29)$$

D. Displacement Power Factor Detection Considering Unbalance Compensation

To obtain the references for DPF compensation considering unbalance compensation, the load current can be represented as

$$i_{jk} = i_{jk}^{p+} + i_{jk}^{Q-} + i_{jk}^- + i_{jk}^0 + i_{jk}^H \quad (30)$$

Where i_{jk}^{p+} , i_{jk}^{Q-} , i_{jk}^- , i_{jk}^0 , and i_{jk}^H are the active positive sequence current, reactive positive sequence current, negative sequence current, zero sequence current, and harmonic current, respectively.

To obtain the instantaneous fundamental positive sequence phase of the currents, $(\phi_{i_{\alpha k}^+})$ the currents are represented in the $\alpha\beta$ frame, that is,

$$\begin{bmatrix} i_{\alpha k}^+ \\ i_{\beta k}^+ \end{bmatrix} = \frac{2}{3} \begin{bmatrix} 1 & -\frac{1}{2} & -\frac{1}{2} \\ 0 & -\frac{\sqrt{3}}{2} & \frac{\sqrt{3}}{2} \end{bmatrix} \begin{bmatrix} i_a^+ \\ i_b^+ \\ i_c^+ \end{bmatrix}. \quad (31)$$

The instantaneous phase is then obtained,

$$\phi_{i_{\alpha k}^+} = \arctan\left(\frac{i_{\alpha k}^+}{i_{\beta k}^+}\right). \quad (32)$$

The same can be done with the fundamental positive sequence voltages $[v_a^+ v_b^+ v_c^+]_k^T$ to obtain the instantaneous phase $\phi_{v_{\alpha k}^+}$.

The quantities involved are similar to those of Fig.8 replacing them with their respective positive sequence quantities. The angle between the fundamental positive sequences voltage and current θ_k^+ is obtained from

$$\theta_k^+ = \phi_{i_{\alpha k}^+} - \phi_{v_{\alpha k}^+} = \theta_{i_{\alpha k}^+} - \theta_{v_{\alpha k}^+}. \quad (33)$$

The fundamental reactive positive sequence current of the load can be evaluated by

$$i_{\alpha k}^{Q-} = A_{i_{\alpha k}^+}^Q \cos(\phi_{v_{\alpha k}^+}) \quad (34)$$

Where

$$A_{i_{\alpha k}^+}^Q = A_{i_{\alpha k}^+} \sin(\theta_k^+) \quad (35)$$

and

$$A_{i_{\alpha k}^+} = A_{i_{\alpha\beta k}^+} = \sqrt{(i_{\alpha k}^+)^2 + (i_{\beta k}^+)^2}. \quad (36)$$

Given a desired displacement power factor DPF, the positive sequence fundamental reactive current associated is

$$A_{i_{\alpha k}^+}^{Qd} = \pm A_{i_{\alpha k}^+} \cos(\theta_k^+) \tan(\arccos(\text{DPF})) \quad (37)$$

Where $A_{i_{\alpha k}^+}^{Qd}$ is positive, if $i_{\alpha k}^+$ leads $v_{\alpha k}^+$, and is negative, if

$i_{\alpha k}^+$ lags $v_{\alpha k}^+$. This equation gives the desired compensated positive sequence fundamental reactive current

$$i_{\alpha k}^{Qd} = A_{i_{\alpha k}^+}^{Qd} \cos(\phi_{v_{\alpha k}^+}) \quad (38)$$

Therefore, from the definition (33) and (34) and (38), the fundamental reactive current reference is

$$i_{j1k}^{Q+ref} = (A_{i_{\alpha k}^+}^Q - A_{i_{\alpha k}^+}^{Qd}) \cos(\phi_{v_{\alpha k}^+}) \quad (39)$$

where the symmetry of the positive sequence components was used and, additionally

$$\phi_{v_{\beta k}^+} = \phi_{v_{\alpha k}^+} - \frac{2\pi}{3}, \quad \phi_{v_{\gamma k}^+} = \phi_{v_{\alpha k}^+} + \frac{2\pi}{3}. \quad (40)$$

Hence, from (20) and (39), the references for displacement power factor compensation with unbalance compensation are given by

$$i_{j1k}^{ref} = i_{j1k}^{ref} + i_{j1k}^{Q+ref}, \quad (41)$$

To compensate harmonics, unbalance, and displacement power factor, (20), (39), and (41), for selective harmonic compensation, or (15), for total harmonic compensation, are used.

Hence,

$$i_{j1k}^{ref} = i_{j1k}^{ref} + i_{j1k}^{ref} + i_{j1k}^{Q+ref} \quad (42)$$

E. Estimation of the PCC State Variables

In real cases, where the system is affected by measuring noises, spikes, and other unpredictable signal disturbances, it is not possible to differentiate a signal x by using the forward approximation $(x_{k+1} - x_k)/T_s$. Therefore, this information has to be filtered. By measuring the PCC voltages and extracting their

harmonic components and quadrature components as described, it is possible to obtain the following relations for the harmonic components of voltage at the PCC $v_{j_{ik}}$ and their respective derivatives $v'_{j_{ik}}$ that constitute state variables of the proposed mathematical model

$$v_{j_{ik}} \approx A_{v_{j_{ik}}} \sin(\omega_k t_k + \theta_{v_{j_{ik}}}) \quad (43)$$

And

$$v'_{j_{ik}} = \omega_k A_{v_{j_{ik}}} \cos(\omega_k t_k + \theta_{v_{j_{ik}}}) \quad (44)$$

where i is the harmonic order of the filtered signal.

6. SYSTEM UNDER STUDY

A. Shunt Active Power Filter

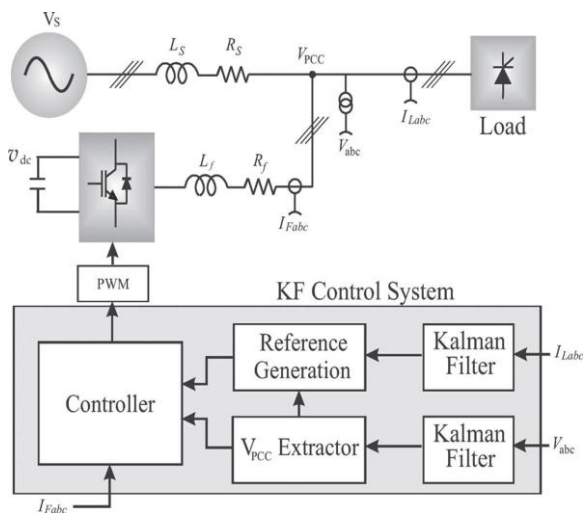


Fig.8.kalman filter based control system for a power quality conditioning device.

B. Series active power filter

The series active power filter compensates current distortion caused by non linear loads. The high impedance imposed by the series APF is created by generating a voltage of the same frequency as that of harmonic component that needs to be eliminated. It acts as a controlled voltage source and can compensate all voltage related problems such as voltage harmonics, voltage sags and swells etc.,

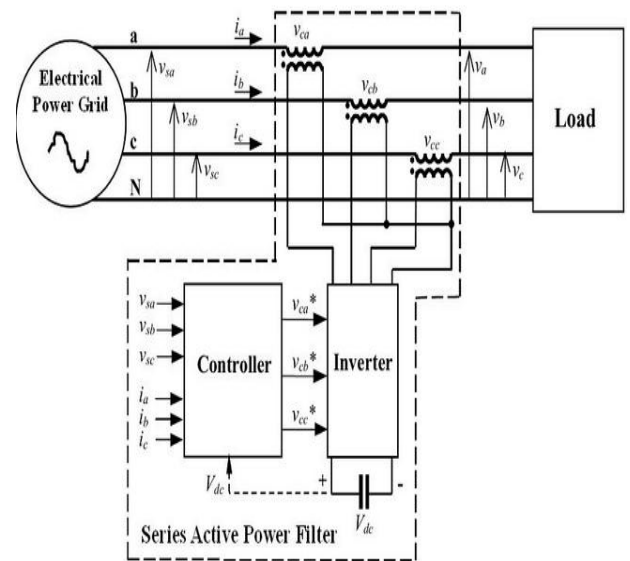


Fig.9.electric diagram of series active power filter

7. RESULTS

A. Shunt Active Power Filter

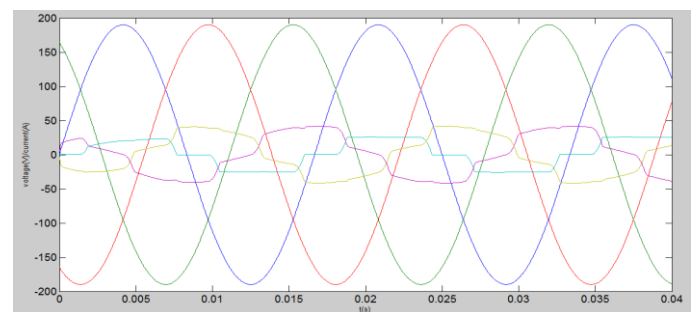


Fig.10.measured grid voltages and load currents.

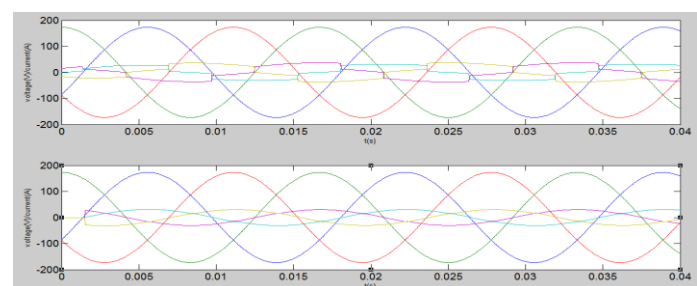


Fig.11. Fundamental voltages and compensated currents. (a) Partial (up to 21st harmonic component) harmonic compensation with unbalance and DPF compensation. (b) Total harmonic compensation with unbalance and DPF compensation

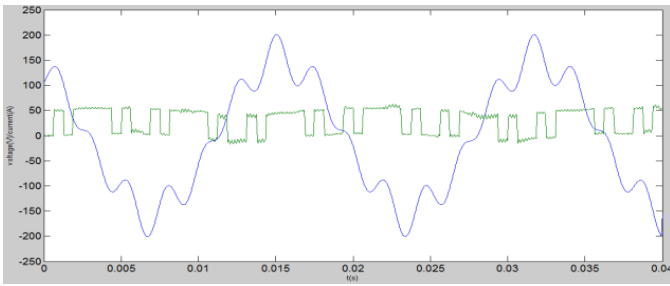


Fig.12. Measured voltage and current..

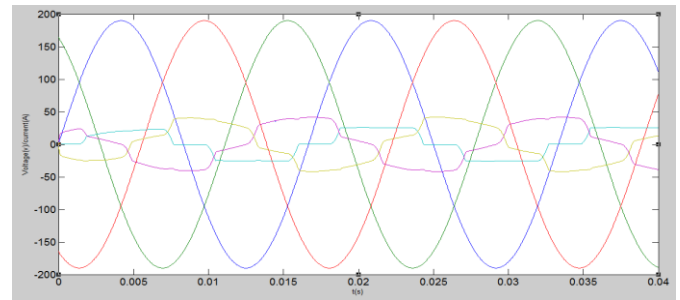


Fig.16.measured grid voltages and load currents

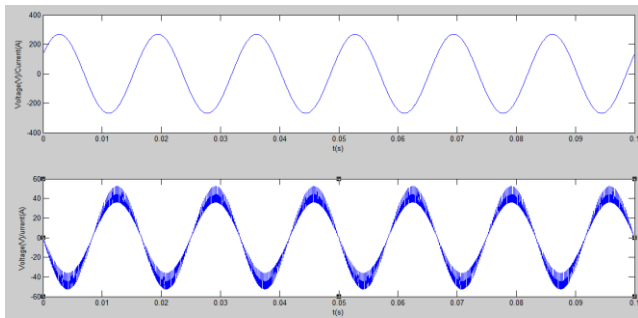


Fig.13. Fundamental voltages and compensated currents. Partial (up to 21st harmonic component) harmonic compensation.

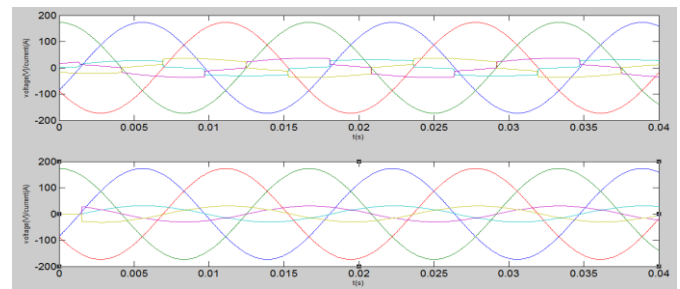


Fig.17. Fundamental voltages and compensated currents. (a) Partial (up to 21st harmonic component) harmonic compensation with unbalance and DPF compensation. (b) Total harmonic compensation with unbalance and DPF compensation.

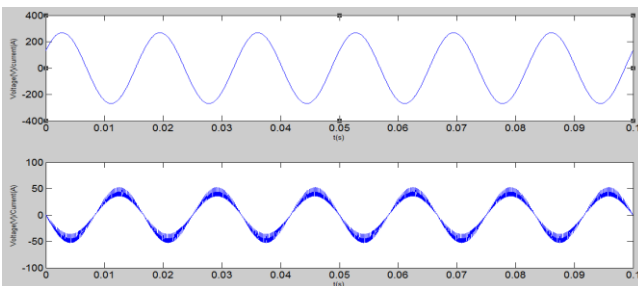


Fig.14. Fundamental voltages and compensated currents. Total (up to 21st harmonic component) harmonic compensation.

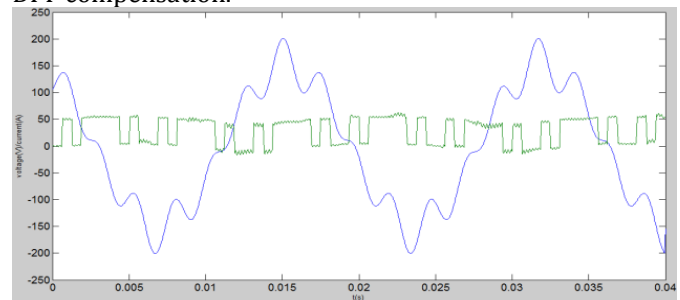


Fig.18. Measured voltage and current..

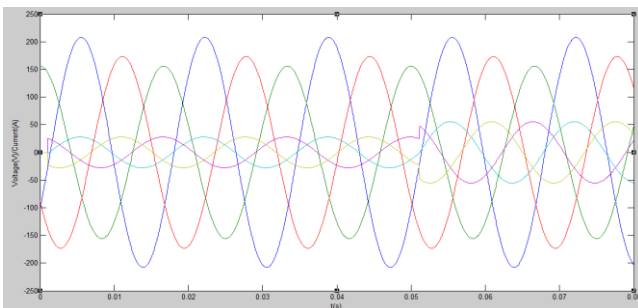


Fig.15. Total harmonic compensation, unbalance compensation of the load currents, and compensation of the positive sequence displacement power factor

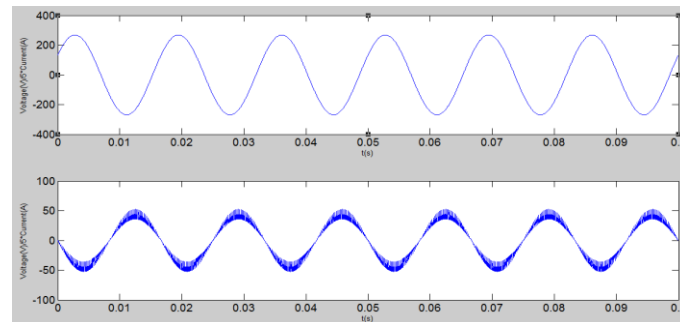


Fig.19. Fundamental voltages and compensated currents. Partial (up to 21st harmonic component) harmonic compensation.

B. Series Active Power Filter

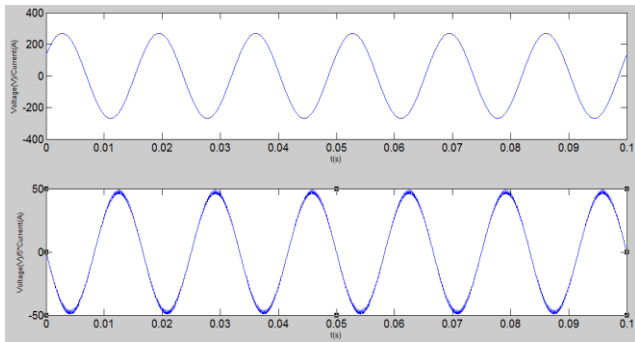


Fig.20. Fundamental voltages and compensated currents. Total (up to 21st harmonic component) harmonic compensation.

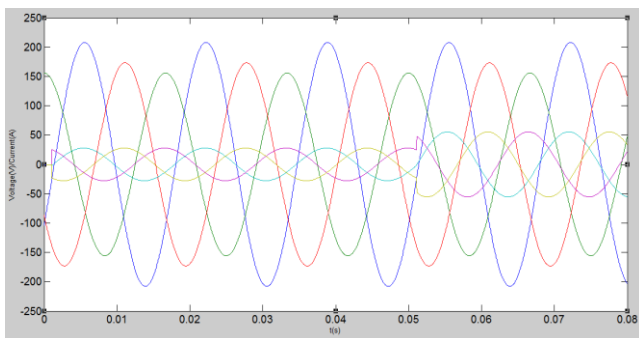


Fig.21. Total harmonic compensation, unbalance compensation of the load currents, and compensation of the positive sequence displacement power factor.

8. CONCLUSION

This paper presented a control system for PQCDs by using KF-based strategy. A complete control algorithm based on optimum theory considering the effects of measurement noise, load currents, and grid voltages transients is proposed. The proposed algorithms generate references for harmonics, unbalance and displacement power factor compensation and can also be implemented in the predictive form. The predictive form is helpful for predictive controllers. The proposed control scheme was designed to present high performance for systems where the line impedance is unknown. A scheme that carries the dynamic information of a distorted voltage signal at the PCC was developed. In the presented algorithm, the state space variables related to the PCC voltages, are estimated and have fast convergence. The results have shown that the developed control structure has a good performance for a huge class of loads, including those with unbalance, showing good tracking behaviour even under high line impedance and frequency deviation.

The proposed method can be implemented in a digital signal processor, reducing the amount of electronic components used in the control circuit.

APPENDIX A

Considering the PCC voltages sinusoidal, balanced and delayed by φ radians, the equations that represent this system are shown below

$$\begin{aligned} v_a &= V \sin(\omega t), \\ v_b &= V \sin(\omega t + \theta), \\ v_c &= V \sin(\omega t - \theta) \end{aligned} \tag{45}$$

Where V is the magnitude of the voltage, $\omega = 2\pi f$ is the angular frequency of the grid, and $\theta = (2\pi/3)\text{rad}$. The first derivatives of this waveforms are shown in (46)

$$\begin{aligned} \frac{dv_a}{dt} &= V\omega \cos(\omega t), \\ \frac{dv_b}{dt} &= V\omega \cos(\omega t + \theta), \\ \frac{dv_c}{dt} &= V\omega \cos(\omega t - \theta). \end{aligned} \tag{46}$$

The second derivatives of (45) are presented in (46)

$$\begin{aligned} \frac{d^2v_a}{dt^2} &= -V\omega^2 \sin(\omega t) \\ \frac{d^2v_b}{dt^2} &= -V\omega^2 \sin(\omega t + \theta) \\ \frac{d^2v_c}{dt^2} &= -V\omega^2 \sin(\omega t - \theta). \end{aligned} \tag{47}$$

From (45)-(47), it is verified that

$\frac{d^2v_{abc}}{dt^2} = -V\omega^2 v_{abc}$. Thus, the complete model that represents the behavior of the voltages at the connection point of the PQCD in the "abc" frame is presented in (48)

$$\begin{bmatrix} \dot{v}_a \\ \dot{v}_b \\ \dot{v}_c \end{bmatrix} = \begin{bmatrix} 0 & 0 & 0 & 1 & 0 & 0 \\ 0 & 0 & 0 & 0 & 1 & 0 \\ 0 & 0 & 0 & 0 & 0 & 1 \\ -\omega^2 & 0 & 0 & 0 & 0 & 0 \\ 0 & -\omega^2 & 0 & 0 & 0 & 0 \\ 0 & 0 & -\omega^2 & 0 & 0 & 0 \end{bmatrix} \begin{bmatrix} v_a \\ v_b \\ v_c \\ \dot{v}_a \\ \dot{v}_b \\ \dot{v}_c \end{bmatrix} \tag{48}$$

With the matrix differentiation property given by(49)

$$\frac{d}{dt} [(C_{abc}^{dq0})^{-1} i_{dq0}] = \frac{d}{dt} (C_{abc}^{dq0})^{-1} + (C_{abc}^{dq0})^{-1} \frac{d}{dt} i_{dq0} \tag{49}$$

Where C_{abc}^{dq0} is the park transform, it is possible to derive the following dq model for fundamental voltages at the connection point:

$$\begin{bmatrix} \dot{v}_d \\ v_q \\ \dot{v}_d \\ \dot{v}_q \end{bmatrix} = \begin{bmatrix} 0 & 0 & 1 & 0 \\ 0 & 0 & 0 & 1 \\ -\omega^2 & 0 & 0 & \omega \\ 0 & -\omega^2 & -\omega & 0 \end{bmatrix} \begin{bmatrix} v_d \\ v_q \\ \dot{v}_d \\ \dot{v}_q \end{bmatrix} \quad (50)$$

APPENDIX B

n- Harmonic Model

Considering the PCC voltages as a sum of ‘n’ harmonic signals as presented in (51)

$$\begin{aligned} v_a &= \sum_{i=1}^n V_i \sin(i\omega t + \theta_{a_i}) \\ v_b &= \sum_{i=1}^n V_i \sin(i\omega t + \theta_{b_i}) \\ v_c &= \sum_{i=1}^n V_i \sin(i\omega t + \theta_{c_i}) \end{aligned} \quad (51)$$

In the same procedure to obtain (46)-(48) and (49) is used to find the matrix $M_{4n \times 4n}^{dq}$, given by (52)

$$M_{4n \times 4n}^{dq} = \begin{bmatrix} 0 & 0 & 1 & 0 & \dots & 0 & 0 & 0 & 0 \\ 0 & 0 & 0 & 1 & \dots & 0 & 0 & 0 & 0 \\ -\omega^2 & 0 & 0 & \omega & \dots & 0 & 0 & 0 & 0 \\ 0 & -\omega^2 & -\omega & 0 & \dots & 0 & 0 & 0 & 0 \\ \vdots & \vdots & \vdots & \vdots & \ddots & \vdots & \vdots & \vdots & \vdots \\ 0 & 0 & 0 & 0 & \dots & 0 & 0 & 1 & 0 \\ 0 & 0 & 0 & 0 & \dots & 0 & 0 & 0 & 1 \\ 0 & 0 & 0 & 0 & \dots & -(n\omega)^2 & 0 & 0 & n\omega \\ 0 & 0 & 0 & 0 & \dots & 0 & -(n\omega)^2 & -n\omega & 0 \end{bmatrix} \quad (52)$$

REFERENCES

[1] P. Verdelho and G. D. Marques, “An active power filter and unbalanced current compensator,” *IEEE Trans. Ind. Electron.*, vol. v. 44, no. 3, pp. 321–328, Jun. 1997.

[2] X. Du, L. Zhou, H. Lu, and H.-M. Tai, “DC link active power filter for three-phase diode rectifier,” *IEEE Trans. Ind. Electron.*, vol. 59, no. 3, pp. 1430–1442, Mar. 2012.

[3] S. Rahmani, A. Hamadi, and K. Al-Haddad, “A Lyapunov-function-based control for a three-phase shunt hybrid active filter,” *IEEE Trans. Ind. Electron.*, vol. 59, no. 3, pp. 1418–1429, Mar. 2012.

[4] S. Dasgupta, S. N. Mohan, S. K. Sahoo, and S. K. Panda, “Lyapunov function-based current controller to control active and reactive power flow from a renewable energy source to a generalized three-phase microgrid system,”

IEEE Trans. Ind. Electron., vol. 60, no. 2, pp. 799–813, Feb. 2013.

[5] F. Ma, A. Luo, X. Xu, H. Xiao, C. Wu, and W. Wang, “A simplified power conditioner based on half-bridge converter for high-speed railway system,” *IEEE Trans. Ind. Electron.*, vol. 60, no. 2, pp. 728–738, Feb. 2013.

[6] H. Akagi, “Control strategy and site selection of a shunt active filter for damping of harmonic propagation in power distribution systems,” *IEEE Trans. Power Del.*, vol. 12, no. 1, pp. 354–363, Jan. 1997.

[7] S. Sangwongwanich and S. Khositkasame, “Design of harmonic current detector and stability analysis of a hybrid parallel active filter,” in *Proc. Power Convers. Conf.*, Nagaoka, Japan, 1997, pp. 181–186.

[8] L. Malesani, P. Mattavelli, and S. Buso, “On the applications of active filters to generic load,” in *Proc. ICHQP*, 1998, pp. 310–319.

[9] G. Escobar, A. A. Valdez, and R. Ortega, “An adaptive controller for a shunt active filter considering load and line impedances,” in *Proc. 11th IEEE Int. Power Electron. Congr.*, 2008, pp. 69–74.

[10] R. Cardoso, R. F. De, Camargo, H. Pinheiro, and H. A. Grünling, “Kalman filter based synchronization methods,” *IET Gener., Transmiss. Distrib.*, vol. 2, no. 4, pp. 542–555, Jul. 2008.

[11] F. Gonzalez-Espin, E. Figueres, and G. Garcera, “An adaptive synchronous-reference-frame phase-locked loop for power quality improvement in a polluted utility grid,” *IEEE Trans. Ind. Electron.*, vol. 59, no. 6, pp. 2718–2731, Jun. 2012.

[12] Y. Tang, P. C. Loh, P. Wang, F. H. Choo, F. Gao, and F. Blaabjerg, “Generalized design of high performance shunt active power filter with output LCL filter,” *IEEE Trans. Ind. Electron.*, vol. 59, no. 3, pp. 1443–1452, Mar. 2012.

BIOGRAPHIES



L.Sreedivika is currently pursuing her M.Tech Degree in Electrical and Electronics Engineering with the specialization in Control Systems From Jawaharlal Nehru Technological University Anantapur, India. She did her B.tech Degree in Electrical and Electronics Engineering from Vaagdevi Institute of technology and science, proddatur, Andhra Pradesh, India 2012.



B.Bhagyamma is currently pursuing her M.Tech degree in Electrical and Electronics Engineering with specialization in Control Systems from Jawaharlal Nehru Technological University, Anantapur, India. She did her B.tech Degree in Electrical and Electronics Engineering from Narayana engineering college, Nellore, Andhra Pradesh, India 2012.